Random-phase approximation with exchange for the photoionization of an atom with an inner open shell

Zhifan Chen and Alfred Z. Msezane

Center for Theoretical Studies of Physical Systems and Department of Physics, Clark Atlanta University, Atlanta, Georgia 30314, USA

(Received 7 May 2007; revised manuscript received 15 January 2008; published 2 April 2008)

A random-phase approximation with exchange method has been developed for the photoionization of atoms (ions) with an inner open shell. The method allows for the inclusion of both intrashell and intershell correlations in the calculation and has been used to study the photoelectron asymmetry parameter and the cross sections of the Sc 4*s* photoionization in which the Sc 3*p*-3*d* transitions have been successfully included. The results demonstrate that the inclusion of the 3*p*-3*d* transitions is extremely important in the intershell coupling, which significantly influences the calculated asymmetry parameter and the cross sections of the Sc 4*s* photoionization. Comparison of our calculated asymmetry parameter and the cross sections with the measured data and available calculation is made and discussed. Possible improvements to the present calculated data are offered as well.

DOI: 10.1103/PhysRevA.77.042703 PACS number(s): 32.80.Fb, 31.15.ve

I. INTRODUCTION

The random-phase approximation with exchange (RPAE) method was first used in the study of atomic physics by Altick and Glassgold [1]. Since then Amusia and Cherepkov [2], Starace [3], and Amusia *et al.* [4] have successfully used the RPAE method in photon-atom collisions for investigating mainly the noble gases and a few other systems. Since the RPAE method was originally developed for closed-shell atoms only, its success with the noble gases has encouraged a generalization of the method to open-shell atoms. Among these methods, the method of [5,6] has the advantage that the RPAE equation reduces to the closed-shell formula for the noble gas atoms and the photoionization cross sections in the length and velocity forms are the same. However, this method cannot calculate the inner-shell photoionization of an atom with an outer open shell and cannot include the intershell correlations in the calculation.

Recently, a RPAE method for two open-shell atoms has been developed by Chen and Msezane [7]. The method has been successfully used to study the inner-shell electron transition of an outer-open-shell atom, such as the $4d$-ϵf photoionization, the so-called giant resonance, of atom I and ions Xe^+ and I^+. However, this method can only include the intrashell correlations. A RPAE method, which allows for the inclusion of both intrashell and intershell correlations has been developed by Chen and Msezane [8] for atoms (ions) with an outer open shell.

In this paper we continue the investigation of the photoionization of open-shell atoms. We will present our RPAE method for the photoionization of an atom with an inner open shell, such as atomic Sc [9–12], in which the inner shells $3p$ and $3d$ and outer shell $4s$ are involved in this calculation. Our method will be used to study the photoelectron angular distribution asymmetry parameter β and the photoionization cross section for the Sc $4s$ electron in the energy region of the $3p$-$3d$ resonance. The results demonstrate the importance of the inclusion of the $3p$-$3d$ transitions in the intershell coupling which was omitted in the previous calculation [10].

II. THEORY

The RPAE equation and the symbols and operators in the equation for an atom with an inner open shell are similar to Eq. (1) of Ref. [8], except that now the $l_1^{n_1}$ is an open shell and $l_2^{n_2}$ is a closed shell. Similar terms should be added in the RPAE equation for the switch of other electron pair. All the matrix elements for the open shell $l_1^{n_1}$ have been derived and implemented in a computer program.

The ground state of the Sc atom has the configuration $[\mathrm{Ar}]3d4s^2(^2D)$. We study the asymmetry parameter for the Sc $4s$ photoionization:

$$h\nu + 3p^6 3d4s^2(^2D) \rightarrow 3p^6 3d4s(^1D,^3D)\epsilon p(^2F,^2P,^2D). \tag{1}$$

Since we have to include all intershell correlations among $3p-\epsilon s, \epsilon d$, $3d-\epsilon p, \epsilon f$, and $4s-\epsilon p$, the following combined core with discrete and continuum electron states have been included in the calculation; a total of 32 channels result:

$$3p^6 3d4s(^1D)\epsilon p(^2D,^2P,^2F),\quad 3p^6 3d4s(^3D)\epsilon p(^2D,^2P,^2F),\quad 3p^5 3d4s^2(^1P)\epsilon s(^2P),$$
$$3p^5 3d4s^2(^1P)\epsilon d(^2D,^2P,^2F),\quad 3p^5 3d4s^2(^1D)\epsilon s(^2D),\quad 3p^5 3d4s^2(^1D)\epsilon d(^2D,^2P,^2F),$$
$$3p^5 3d4s^2(^1F)\epsilon s(^2F),\quad 3p^5 3d4s^2(^1F)\epsilon d(^2D,^2P,^2F),\quad 3p^5 3d4s^2(^3P)\epsilon s(^2P),\quad 3p^5 3d4s^2(^3P)\epsilon d(^2D,^2P,^2F),$$
$$3p^5 3d4s^2(^3D)\epsilon s(^2D),\quad 3p^5 3d4s^2(^3D)\epsilon d(^2D,^2P,^2F),\quad 3p^5 3d4s^2(^3F)\epsilon s(^2F),$$
$$3p^5 3d4s^2(^3F)\epsilon d(^2D,^2P,^2F),\quad 3p^6 4s^2(^1S)\epsilon f(^2F),\quad 3p^6 4s^2(^1S)\epsilon p(^2P).$$

The closed shells of $1s$, $2s$, $2p$, and $3s$ are not listed above. As the $3p$-$3d$ resonance will greatly affect the $4s$ photoionization, therefore in addition to these channels our code has several special subroutines to treat the Sc $3p$-$3d$ transitions, a total of nine channels:

$$3p^6 3d 4s^2(^2D) + h\nu \rightarrow 3p^5 3d^2(^1D, ^1S, ^3P)4s^2(^2P), \quad (2)$$

$$3p^6 3d 4s^2(^2D) + h\nu \rightarrow 3p^5 3d^2(^1D, ^3P, ^3F)4s^2(^2D), \quad (3)$$

$$3p^6 3d 4s^2(^2D) + h\nu \rightarrow 3p^5 3d^2(^1D, ^1G, ^3F)4s^2(^2F). \quad (4)$$

The final states in Eqs. (2)–(4) have been obtained through self-consistent Hartree-Fock (HF) calculations. The parameters, which are needed in the RPAE calculation, were assigned to the excited $3d$ electron. The calculation involves a total 41 channels (14 ^2P, 14 ^2F, and 13 ^2D) in the intershell coupling. The dipole and Coulomb matrix elements for the Sc photoionization without the inclusion of the $3p$-$3d$ transitions are given in Appendix A. The Coulomb matrix elements involved in the Sc $3p$-$3d$ transitions are listed in Appendix B.

The asymmetry parameter for the Sc $4s$ photoionization can be evaluated through

$$\beta = \frac{2|S(0)|^2 - 3|S(1)|^2 + |S(2)|^2}{|S(0)|^2 + 3|S(1)|^2 + 5|S(2)|^2}, \quad (5)$$

where $S(j_t)$ is the scattering amplitude which can be evaluated for Sc $4s$ photoionization from

$$S(j_t) = B\sum_{L'} (-1)^{L'}(2L'+1)^{1/2} \exp(-i\delta_l^{L_c S_c L'})\langle L'S'\|D\|LS\rangle \times \begin{Bmatrix} L & j_t & L_c \\ l & L' & k \end{Bmatrix}. \quad (6)$$

In Eq. (6), L, L_c, and L' represent, respectively the quantum numbers of the orbital angular momentum of the atom, the ion after photoionization, and the ion plus photoelectron, $\delta_l^{L_c S_c L'}$ is the photoelectron phase shift with respect to Coulomb waves, j_t is the angular momentum transferred, l is the orbital angular momentum of the photoelectron, B will be canceled from the denominator and numerator in Eq. (5), $k=1$ for the dipole calculation, and $\langle L'S'\|D\|LS\rangle$ is the dipole matrix element in RPAE.

After evaluating the dipole and Coulomb matrix elements, the RPAE equation was solved for the partial cross sections of ^2P, ^2D, and ^2F final-state terms. In the calculation we used the binding energies from Tables I and II of Ref. [10] for the Sc $3p$, $3d$, and $4s$ electrons. For the $3p$-$3d$ transitions the resonance energies were taken also from Ref. [10], except the energies resulting from the state $3p^5 3d^2(^1G, ^3F)4s^2(^2F)$; these were taken from Refs. [9,11].

III. RESULTS

Figure 1 gives the asymmetry parameter β for the Sc $4s$ photoionization leading to the Sc^+ ionic term ^3D. The solid curve and the dash-dotted curve in Fig. 1 represent, respectively the length and velocity forms of the β values obtained with the inclusion of the $3p$-$3d$ transitions, Eqs. (2)–(4). The dotted curve shows the experimental data [9]. The dashed curve is the length form of the β value obtained without the $3p$-$3d$ transitions. There are three deep minima in the dashed line. Also, the solid curve exhibits six deep minimum regions. From the dashed curve we found the β values to be between 1.84 and 1.98, which are close to 2, if the photon energy is less than about 37.5 eV. This can be understood by analyzing Eq. (6). A coefficient A can be defined for the parameters of Eq. (6),

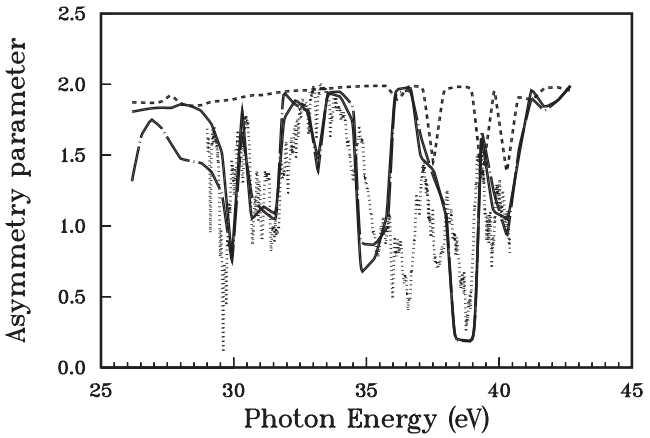

FIG. 1. Comparison of our RPAE results with the experimental data for the Sc $4s$ asymmetry parameter of the Sc^+ ionic term ^3D. Solid and dash-dotted curves represent, respectively, the length and velocity forms of the β value with the inclusion of the $3p$-$3d$ transitions in the intershell coupling. The dotted curve is taken from the experimental data [9]. The dashed curve is the length form of the β values without inclusion of the $3p$-$3d$ transitions.

$$A = (-1)^{L'}(2L'+1)^{1/2} \begin{Bmatrix} L & j_t & L_c \\ l & L' & k \end{Bmatrix},$$

which is not a function of the photon energy. The β value is determined by the A's, the relative values of the phase, and the dipole matrix elements in RPAE. As the energy region of the $3p$-$3d$ resonance is much higher than the $4s$ ionization energy, the phases will not affect much the β value. The β value will mainly be determined by the dipole matrix elements in RPAE and the A's. We found that two A's always have different signs for $j_t=1$ and 2, so the dipole matrix elements in RPAE will partly cancel out with each other. Finally $S(0)^2 \gg S(1)^2$ and $S(2)^2$—i.e., the anisotropic interaction—is small between the departing electron and the ion, so β is close to 2. The above analysis shows that the β minimum should occur at the place where the three dipole matrix elements have large differences.

Figure 2 displays the dipole matrix elements in RPAE versus the photon energy for the Sc^+ ionic term ^3D when the $3p$-$3d$ transitions are involved. Solid, dashed, and dotted curves in Fig. 2 represent, respectively the dipole matrix elements in RPAE for the final state terms ^2P, ^2D, and ^2F. Since the square of the dipole matrix element in RPAE is equal to the square of the real part plus the square of the imaginary part, the dipole matrix element in RPAE is the

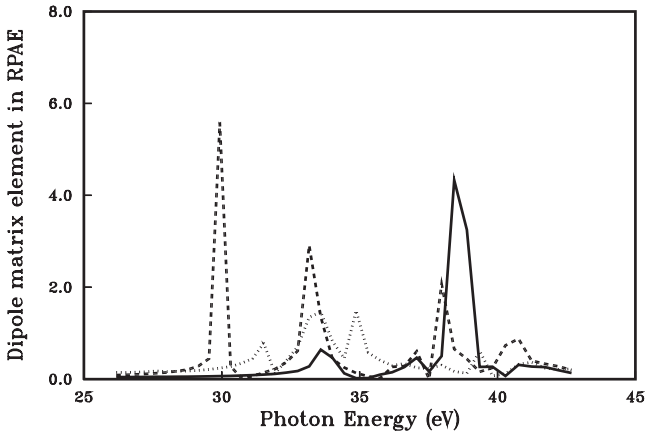

FIG. 2. The dipole matrix element calculated in the length form of the RPAE versus photon energy when the $3p$-$3d$ transition is involved in the intershell coupling. Solid, dashed, and dotted curves represent, respectively, the final state terms ^2P, ^2D, and ^2F.

square root of the result; it is always positive. By comparing the data in Figs. 1 and 2 we found the first (29.92 eV) and third (33.17 eV) minima of β to correspond to the maxima of the dipole matrix elements for the final term ^2D. The second (31.52 eV) and fourth (34.87–35.1 eV) minima of the solid curve correspond to the maxima of the dipole matrix elements of the final term ^2F. The fifth minimum (38.42–38.88 eV) of the solid curve in Fig. 1 is caused by the maximum of the dipole matrix elements of the final ^2P term. The sixth minimum of β is near the ^2D maximum in Fig. 2 at 40.76 eV. Those maxima of the dipole matrix elements are caused mainly by the intershell coupling between the states $3p^6 3d 4s(^3D)\epsilon p(^2P, ^2D, ^2F)$ and $3p^5 3d^2(^1D, ^1S, ^3P, ^3F, ^1G)$ $4s^2(^2P, ^2D, ^2F)$.

Figure 3 gives the photoelectron angular distribution asymmetry parameter β for the Sc^+ ionic term ^1D. The curves have the same meaning as in Fig. 1. The solid curve matches the basic structure of the experimental curve. A similar analysis of the β minima can be done for the curves. For example, the first minimum of the β is caused by the maximum of the dipole matrix elements for the ^2D final term at 29.82 eV. The second to fifth minima are near the maxima

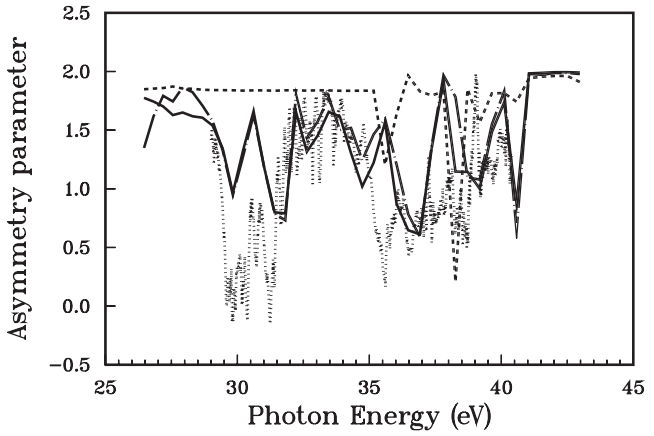

FIG. 3. Same as in Fig. 1, except that the data are for the Sc^+ ionic term ^1D.

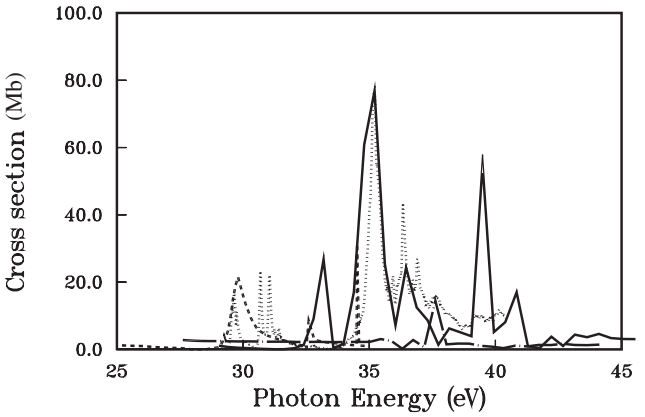

FIG. 4. The photoionization cross section for the Sc $3d$ electron. Dotted and dashed curves are, respectively, from the measurement [9] and previous calculation [10]. The solid curve represents our RPAE calculation shifted by 1.43 eV to match the experimental maximum.

of the dipole matrix elements for the final term ^2F.

The solid, dashed, and dotted curves in Figs. 1 and 3 demonstrate the importance of including the $3p$-$3d$ transitions in the intershell coupling.

The Sc photoionization cross sections have also been calculated. The results are given in Figs. 4–6. Figure 4 shows the photoionization cross sections for the Sc $3d$-$\epsilon p, \epsilon f$ transitions versus photon energy. The dotted and dashed curves represent, respectively, the experimental data [9] and the previous calculation [10]. The dotted curve in Fig. 4 as stated in Ref. [9] was used to normalize the Sc $4s$ photoionization. At 35.24 eV the intensity of the $3d$-$\epsilon p, \epsilon f$ transitions was arbitrarily set to 100 in the measurement. Then, the intensities of the $4s$ photoionization leading to the Sc^+ ionic terms ^3D and ^1D were 15.6. These relative intensities can be normalized to the absolute value using our RPAE calculation. The peak of our cross section for the Sc $3d$-$\epsilon p, \epsilon f$ transitions is around 33.78 eV. To match the experimental maximum at 35.21 eV the theoretical result was shifted by 1.43 eV and is

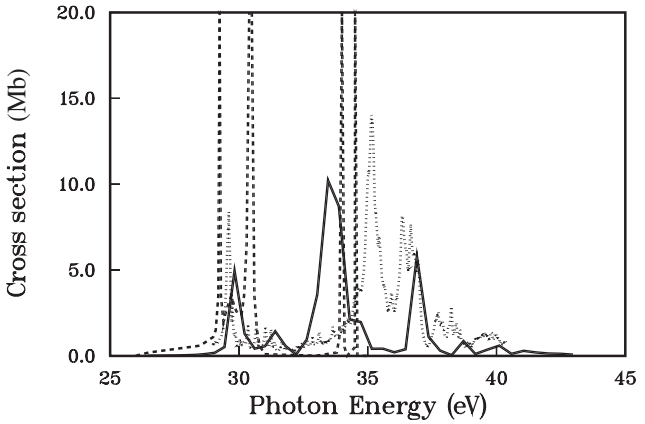

FIG. 5. The photoionization cross section for the Sc $4s$ electron leading to the Sc^+ ionic term ^1D. Curves have the same meaning as in Fig. 4.

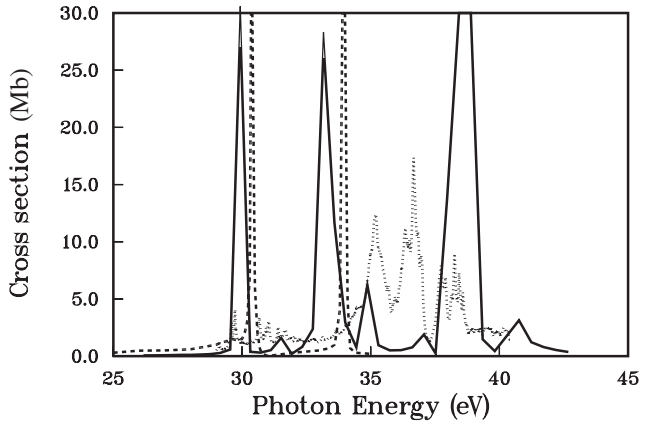

FIG. 6. Same as Fig. 5, but for the Sc^+ ionic term ^3D.

represented by the solid curve in Fig. 4. The solid curves in Figs. 5 and 6 have also been shifted by the same value. The experimental maximum at 35.21 eV now has the cross-section value of 76.81 Mb. This maximum is caused by the intershell coupling between (i) the $3p^64s^2(^1S)\epsilon f(^2F)$ and $3p^53d^2(^1G,^3F)4s^2(^2F)$ and (ii) the $3p^64s^2(^1S)\epsilon p(^2P)$ and $3p^53d^2(^1S)4s^2(^2P)$. The dash-dotted curve in the Fig. 4 which is near the horizontal axis is from our calculation without the inclusion of the $3p$-$3d$ transitions. These cross sections are very small in comparison with the experimental data and will not be drawn in Figs. 5 and 6.

The photoionization cross sections for the Sc $4s$ electron leading to the Sc^+ ionic terms ^1D and ^3D are, respectively, given in Figs. 5 and 6. The curves have the same meaning as in Fig. 4. In Fig. 5 the measurement [9] shows a maximum at 35.14 eV while the solid curve has a maximum at 34.89 eV. This maximum is caused by the following intershell coupling: (i) the $3p^63d4s(^1D)\epsilon p(^2P)$ and $3p^53d^2(^1S)4s^2(^2P)$, (ii) the $3p^63d4s(^1D)\epsilon p(^2D)$ and $3p^53d^2(^3P)4s^2(^2D)$, and (iii) the $3p^63d4s(^1D)\epsilon p(^2F)$ and $3p^53d^2(^1G,^3F)4s^2(^2F)$. In Fig. 6 the experimental cross sections have maxima around 35.19 eV and 36.67 eV. There are four maxima around 31.36 eV, 34.66 eV, 36.30 eV, and 39.86 eV from our calculation. The first two maxima are caused mainly by the coupling between the $3p^63d4s(^3D)\epsilon p(^2D)$ and $3p^53d^2(^1D)4s^2(^2D)$. A small part is contributed by the coupling between the $3p^63d4s(^3D)\epsilon p(^2F)$ and $3p^53d^2(^1G,^3F)4s^2(^2F)$. The third and final large maxima are caused, respectively, almost totally by the coupling between the $3p^63d4s(^3D)\epsilon p(^2F)$ and $3p^53d^2(^1G,^3F)4s^2(^2F)$ and the $3p^63d4s(^3D)\epsilon p(^2P)$ and $3p^53d^2(^3P)4s^2(^2P)$. As seen from Fig. 6 the experimental maxima are much smaller than the theoretical results.

Figures 4–6 show our improved results for the Sc $3d,4s$ photoionization cross sections, with also the discrepancy. Reference [9] has analyzed the large discrepancy in comparison with the calculation [10]. According to our calculation the main reason for the large discrepancy between the data of Ref. [10], dashed curves in Figs. 5 and 6, and the results of Ref. [9], dotted curves, is that the calculation [10] did not open the $3p$-$3d$ transition channels and include them in the intershell coupling. The discrepancy between our calculation and that of Ref. [9]. suggests a more careful measurement and analysis of the location of the nine Sc $3p$-$3d$ resonances. To date, there are arguments about the resonance energies for these transitions [9–12]. From our calculation it seems there is a resonance located around 36–38 eV. Other improvements to the current calculation are also worth trying, such as adding correlations to the initial state as well as including relativistic effects and spin-orbit interaction to the wave function. The two electron processes are probably also very important [12].

IV. CONCLUSION

In conclusion, we have developed a RPAE method for an atom with an inner open shell. The method has been used to study the asymmetry parameter β and the cross section for the Sc $4s$ photoionization with inclusion of the $3p$-$3d$ transitions. The results show improved agreement with the experimental data and demonstrate the importance of including the Sc $3p$-$3d$ transitions in the intershell coupling. There is scope for improvement of the calculation as indicated above.

ACKNOWLEDGMENTS

This work was supported by the U.S. DOE, Division of Chemical Sciences, Geosciences and Biosciences, Office of Basic Energy Sciences, OER. The authors thank Professor Scott Whitfield for providing them the experimental data.

APPENDIX A: DIPOLE AND COULOMB MATRIX ELEMENTS FOR Sc PHOTOIONIZATION

In the following equations $l_1^{n_1}$ is an open shell and the other l^n subshells are closed shells. $G_{L_1S_1}^{L_1'S_1'}$, etc., is the fractional parentage coefficient [13].

For the transition

$$|l_1^{n_1}[L_1S_1]l_2^{n_2}[L_2S_2]LS\rangle \rightarrow |l_1^{n_1}[L_1S_1]l_2^{n_2-1}[L_2'S_2']l_5L'S'\rangle, \tag{A1}$$

the reduced dipole matrix element is

$$\langle L'S'|O^k|LS\rangle = \langle l_5\|C^k r\|l_2\rangle(-1)^{n_1+L'+k+L+3S_c'+S_1+1/2} \times \frac{[L'L_c'S_c']^{1/2}}{[S_1]^{1/2}} \begin{Bmatrix} l_2 & k & l_5 \\ L' & L_c' & L \end{Bmatrix}.$$

For the Coulomb interaction

$$|l_1^{n_1}[L_1S_1]l_2^{n_2-1}[L_2'S_2']l_5L'S'\rangle \rightarrow |l_1^{n_1}[L_1S_1]l_2^{n_2-1}[L_2''S_2'']l_6L''S''\rangle, \tag{A2}$$

the Coulomb matrix element of time forward type is

$$\sum_k \frac{[L_c' S_c' L_c'' S_c'']^{1/2}}{[S_1][L_1]^{1/2}} \begin{Bmatrix} l_5 & k & l_2 \\ L_1 & L_c' & L' \end{Bmatrix} \begin{Bmatrix} l_2 & k & l_6 \\ L'' & L_c'' & L_1 \end{Bmatrix} \langle l_6 \| C^k \| l_2 \rangle \langle l_2 \| C^k \| l_5 \rangle R_k(l_6 l_2; l_2 l_5) (-1)^{S_c'+3S_c''+l_2+l_6} \delta_{S'=S} - \sum_k [L_c'' L_c']^{1/2} \begin{Bmatrix} L_c'' & l_6 & L'' \\ l_5 & L_c' & k \end{Bmatrix}$$
$$\times \begin{Bmatrix} l_2 & k & l_2 \\ L_c'' & L_1 & L_c' \end{Bmatrix} \langle l_6 \| C^k \| l_5 \rangle \langle l_2 \| C^k \| l_2 \rangle R_k(l_6 l_2; l_5 l_2) (-1)^{L_c''+L_c'+L_1+L'+l_2+l_6} \delta_{S_c'=S_c''}.$$

The exchange part of the Coulomb matrix element of time backward type is

$$-\sum_k [L_c' S_c' L_c'' S_c'']^{1/2} \begin{Bmatrix} L'' & L_c'' & l_6 \\ L_c' & L_1 & l_2 \\ l_5 & l_2 & k \end{Bmatrix} \begin{Bmatrix} S_c' & 1/2 & S' \\ S_c'' & 1/2 & S_1 \end{Bmatrix} \langle l_6 \| C^k \| l_2 \rangle \langle l_5 \| C^k \| l_2 \rangle R_k(l_6 l_5; l_2 l_2) (-1)^{L_c'+3S_c'+L_c''+3S_c''},$$

where the symbol $\{\cdots\}$ with three lines is the so-called $9j$ symbol.

For the Coulomb interaction

$$|l_1^{n_1-1}[L_1' S_1'] l_2^{n_2} [L_2 S_2][L_c'' S_c''] l_5 L' S' \rangle \to |l_1^{n_1}[L_1 S_1] l_2^{n_2-1}[L_2' S_2'][L_c' S_c'] l_6 L'' S'' \rangle, \tag{A3}$$

the Coulomb matrix element of time forward type is

$$\sum_k G^{L_1 S_1}_{L_1' S_1'} \sqrt{n_1} \frac{[L_1, L_c', S_c']^{1/2}}{[S']^{1/2}} \begin{Bmatrix} l_1 & l_5 & k \\ L'' & L_1 & L_c'' \end{Bmatrix} \begin{Bmatrix} l_6 & l_2 & k \\ L_1 & L' & L_c' \end{Bmatrix} \langle l_6 \| C^k \| l_2 \rangle \langle l_1 \| C^k \| l_5 \rangle R_k(l_6 l_1; l_2 l_5) (-1)^{l_5+L_1'+S'+3S_c'+L+1/2}$$
$$- \sum_k G^{L_1 S_1}_{L_1' S_1'} \sqrt{n_1} \frac{[L_1, L_c', S_1]^{1/2}}{[S_c']^{1/2}} \begin{Bmatrix} L_c' & l_6 & L' \\ l_5 & L_c'' & k \end{Bmatrix} \begin{Bmatrix} l_1 & k & l_2 \\ L_c' & L & L_c'' \end{Bmatrix} \langle l_6 \| C^k \| l_5 \rangle \langle l_1 \| C^k \| l_2 \rangle R_k(l_6 l_1; l_5 l_2) (-1)^{l_2+L'+3S'+L_c'+S_1'+3/2+l_1+l_6} \delta_{S_c'=S_c''}.$$

The exchange part of the Coulomb matrix element of time backward type is

$$-\sum_k G^{L_1 S_1}_{L_1' S_1'} \sqrt{n_1} [L_c', S_c', L_1, S_1]^{1/2} \begin{Bmatrix} L' & L_c' & l_6 \\ L_1' & L & l_1 \\ l_5 & l_2 & k \end{Bmatrix} \begin{Bmatrix} S_c' & 1/2 & S' \\ S_1' & 1/2 & S \end{Bmatrix} \langle l_6 \| C^k \| l_1 \rangle \langle l_5 \| C^k \| l_2 \rangle R_k(l_6 l_5; l_1 l_2) (-1)^{3S_1+3S_c'+l_1+L_c'+L_1+3/2}.$$

For the Coulomb interaction

$$|l_3^{n_3-1}[L_3' S_3'] l_1^{n_1}[L_1 S_1] l_2^{n_2}[L_2 S_2][L_c'' S_c''] l_5 L'' S'' \rangle \to |l_3^{n_3}[L_3 S_3] l_1^{n_1-1}[L_1 S_1] l_2^{n_2-1}[L_2' S_2'][L_c' S_c'] l_6 L' S' \rangle, \tag{A4}$$

the Coulomb matrix element of time forward type is

$$\sum_k \frac{[L_c'', S_c'', L_c', S_c']^{1/2}}{[S']} \begin{Bmatrix} l_3 & l_5 & k \\ L'' & L & L_c'' \end{Bmatrix} \begin{Bmatrix} l_6 & l_2 & k \\ L & L' & L_c' \end{Bmatrix} \langle l_3 \| C^k \| l_5 \rangle \langle l_6 \| C^k \| l_2 \rangle R_k(l_6 l_3; l_2 l_5) (-1)^{L+n_1+l_5+L_c''+3S+3/2+S_c'+l_6+l_3}$$
$$- \sum_k [L_c', L_c'']^{1/2} \begin{Bmatrix} L_c' & l_6 & L' \\ l_5 & L_c'' & k \end{Bmatrix} \begin{Bmatrix} l_2 & l_3 & k \\ L_c'' & L_c' & L_1 \end{Bmatrix} \langle l_6 \| C^k \| l_5 \rangle \langle l_3 \| C^k \| l_2 \rangle R_k(l_6 l_3; l_2 l_5) (-1)^{n_1+L'+3S_1+l_2+L_c'+S_c'+3/2+l_3+l_6} \delta_{S_c''=S_c'}.$$

The exchange part of the Coulomb matrix element of time backward type is

$$-\sum_k [L_c'', S_c'', L_c', S_c']^{1/2} \begin{Bmatrix} L' & L_c' & l_6 \\ L_c'' & L & l_3 \\ l_5 & l_2 & k \end{Bmatrix} \begin{Bmatrix} S_c' & 1/2 & S' \\ S_c'' & 1/2 & S \end{Bmatrix} \langle l_6 \| C^k \| l_2 \rangle \langle l_5 \| C^k \| l_3 \rangle R_k(l_6 l_5; l_2 l_3) (-1)^{n_1+L_c'+S_c'+2S_c''+l_3+L_1+3/2+3S_1}.$$

APPENDIX B: THE COULOMB MATRIX ELEMENTS INVOLVING THE Sc 3*p*-3*d* TRANSITIONS

For the Coulomb interaction

$$|l_3^{n_3-1}[L_3' S_3'] l_1^{n_1+1}[L_1'' S_1''] L'' S'' \rangle \to |l_3^{n_3-1}[L_3' S_3'] l_1^{n_1+1}[L_1' S_1'] L' S' \rangle, \tag{B1}$$

the Coulomb matrix element of time forward type is

$$\sum_{k\bar{L}} G^{L_1''S_1''}_{\bar{L}S} G^{L_1'S_1'}_{\bar{L}S} \frac{[L_1'',S_1'',L_1',S_1']^{1/2}(n_1+1)}{[S']} \begin{Bmatrix} l_1 & l_3 & k \\ L'' & \bar{L} & L_1'' \end{Bmatrix} \begin{Bmatrix} l_3 & l_1 & k \\ \bar{L} & L' & L_1' \end{Bmatrix} \langle l_1\|C^k\|l_3\rangle\langle l_3\|C^k\|l_1\rangle R_k(l_1l_3;l_1l_3)(-1)^{2S'+2S_1''+l_3+L_1''+l_1+L_1'+1}$$

$$-\sum_{k} [L_1'',L_1']^{1/2}(n_1+1) G^{L_1''S_1''}_{\bar{L}S} G^{L_1'S_1'}_{\bar{L}S} \begin{Bmatrix} l_1 & l_1 & k \\ L_1'' & L_1' & \bar{L} \end{Bmatrix} \begin{Bmatrix} l_3 & L_1' & L' \\ L_1'' & l_3 & k \end{Bmatrix} \langle l_3\|C^k\|l_3\rangle\langle l_1\|C^k\|l_1\rangle R_k(l_3l_3;l_1l_1)(-1)^{L''+2S'+2S_1'+l_1+l_3+\bar{L}}\delta_{S_1''=S_1'}.$$

The exchange part of the Coulomb matrix element of time backward type is

$$-\sum_{kL_c''L_c'S_c''S_c'} G^{L_1'S_1'}_{L_1S_1} G^{L_1''S_1''}_{L_1S_1} [L_c'',S_c'',L_c',S_c'][L_1'',S_1'',L_1',S_1']^{1/2}(n_1+1) \begin{Bmatrix} L' & L_c' & l_1 \\ L_c'' & L & l_3 \\ l_1 & l_3 & k \end{Bmatrix} \begin{Bmatrix} S_c' & 1/2 & S' \\ S_c'' & 1/2 & S_1 \end{Bmatrix} \begin{Bmatrix} S_1'' & 1/2 & S'' \\ S_c'' & 1/2 & S_1 \end{Bmatrix} \begin{Bmatrix} S_1' & 1/2 & S' \\ S_c' & 1/2 & S_1 \end{Bmatrix}$$

$$\times \begin{Bmatrix} L_1'' & L'' & l_3 \\ L_c'' & L_1 & l_1 \end{Bmatrix} \begin{Bmatrix} L_1' & L' & l_3 \\ L_c' & L_1 & l_1 \end{Bmatrix} \langle l_1\|C^k\|l_3\rangle\langle l_1\|C^k\|l_3\rangle R_k(l_1l_1;l_3l_3)(-1)^{2S_c'+2S_c''+2S'+1},$$

where $L_c''S_c''$ are defined in the state of $l_3^{n_3-1}[L_3'S_3']l_1''^{n_1}[L_1S_1][L_c''S_c'']$. The same $L_c''S_c''$ are used in Eqs. (B2)–(B4).

For the Coulomb interaction

$$|l_3^{n_3-1}[L_3'S_3']l_1''^{n_1+1}[L_1'S_1']l_2''^{n_2}[L_2S_2]L''S''\rangle \to |l_3''^{n_3}[L_3S_3]l_1''^{n_1}[L_1S_1]l_2''^{n_2-1}[L_2'S_2'][L_c'S_c']l_6L'S'\rangle, \tag{B2}$$

the Coulomb matrix element of time forward type is

$$\sum_{k\bar{L}} G^{L_1'S_1'}_{\bar{L}S} \frac{[L_c',S_c',L_1',S_1']^{1/2}\sqrt{n_1+1}}{[S']} \begin{Bmatrix} l_6 & l_2 & k \\ \bar{L} & L' & L_c' \end{Bmatrix} \begin{Bmatrix} l_1 & l_3 & k \\ L'' & \bar{L} & L_1' \end{Bmatrix} \langle l_6\|C^k\|l_2\rangle\langle l_3\|C^k\|l_1\rangle R_k(l_6l_3;l_1l_2)(-1)^{S+1/2+S_c'+L''+2S_1'+l_6+L_1'+n_1+k}$$

$$-\sum_{k} [L_1',S_1',L_c',S_c']^{1/2}[L'](n_1+1) G^{L_1'S_1'}_{LS} \begin{Bmatrix} l_2 & L_1 & L_c' \\ l_6 & L' & L' \end{Bmatrix} \begin{Bmatrix} l_2 & L' & L' \\ L_1' & l_3 & k \end{Bmatrix} \begin{Bmatrix} l_6 & l_1 & k \\ L_1' & L' & L \end{Bmatrix} \begin{Bmatrix} 1/2 & S_1 & S_c' \\ 1/2 & S' & S_1' \end{Bmatrix} \langle l_6\|C^k\|l_1\rangle$$

$$\times\langle l_3\|C^k\|l_2\rangle R_k(l_6l_3;l_2l_1)(-1)^{1/2+L_c'+S_c'+2S_1'+l_1+l_2+l_3+L_1+3S'}.$$

The exchange part of the Coulomb matrix element of time backward type is

$$-\sum_{kL_c''S_c''} G^{l_1''^{n_1+1}[L_1'S_1']}_{l_1''^{n_1}[L_1S_1]} [L_c'',S_c''][L_c',S_c',L_1',S_1']^{1/2}\sqrt{n_1+1} \begin{Bmatrix} L' & L_c' & l_6 \\ L_c'' & L & l_3 \\ l_1 & l_2 & k \end{Bmatrix} \begin{Bmatrix} S_c' & 1/2 & S' \\ S_c'' & 1/2 & S \end{Bmatrix} \begin{Bmatrix} S_1' & 1/2 & S'' \\ S_c'' & 1/2 & S_1 \end{Bmatrix} \begin{Bmatrix} L_1' & L'' & l_3 \\ L_c'' & L_1 & l_1 \end{Bmatrix} \langle l_6\|C^k\|l_3\rangle$$

$$\times\langle l_1\|C^k\|l_2\rangle R_k(l_1l_6;l_2l_3)(-1)^{S_c'+2S_c''+1/2+n_1+L_c'+L''+l_1+S''}.$$

For the Coulomb interaction

$$|l_3^{n_3-1}[L_3'S_3']l_1''^{n_1+1}[L_1'S_1']l_2''^{n_2}[L_2S_2]L''S''\rangle \to |l_3''^{n_3-1}[L_3S_3]l_1''^{n_1}[L_1S_1]l_2''^{n_2}[L_2S_2][L_c'S_c']l_6L'S'\rangle, \tag{B3}$$

the Coulomb matrix element of time forward type is

$$\sum_{k} G^{L_1'S_1'}_{L_1S_1} \frac{[L_c',S_c',L_1',S_1']^{1/2}\sqrt{n_1+1}}{[S']} \begin{Bmatrix} l_6 & l_3 & k \\ L & L' & L_c' \end{Bmatrix} \begin{Bmatrix} l_1 & l_3 & k \\ L'' & L & L_1' \end{Bmatrix} \langle l_6\|C^k\|l_3\rangle\langle l_3\|C^k\|l_1\rangle R_k(l_6l_3;l_1l_3)(-1)^{L'+2S_1'+L_1'+L_1+L_c'+2S_c'+k}$$

$$-\sum_{k\bar{L}} [L_1',S_1',L_c',S_c']^{1/2}[\bar{L}]\sqrt{n_1+1} G^{L_1'S_1'}_{L_1S_1} \begin{Bmatrix} l_2 & l_3 & k \\ L'' & \bar{L} & L_1' \end{Bmatrix} \begin{Bmatrix} l_6 & l_1 & k \\ \bar{L} & L' & L_c' \end{Bmatrix} \begin{Bmatrix} 1/2 & S_1 & S_c' \\ 1/2 & S' & S_1' \end{Bmatrix} \begin{Bmatrix} L_1 & L_c' & l_3 \\ \bar{L} & L_1' & l_1 \end{Bmatrix} \langle l_6\|C^k\|l_1\rangle$$

$$\times\langle l_3\|C^k\|l_3\rangle R_k(l_6l_3;l_3l_1)(-1)^{L'+L_1'+2S'+2S_c'+2S_1'+L_c'+L_1+k+1}.$$

The exchange part of the Coulomb matrix element of time backward type is

$$-\sum_{kL_c''S_c''} G^{l_1''^{n_1+1}[L_1'S_1']}_{l_1''^{n_1}[L_1S_1]} [L_c'',S_c''][L_c',S_c',L_1',S_1']^{1/2}\sqrt{n_1+1} \begin{Bmatrix} L' & L_c' & l_6 \\ L_c'' & L & l_3 \\ l_1 & l_3 & k \end{Bmatrix} \begin{Bmatrix} S_c' & 1/2 & S' \\ S_c'' & 1/2 & S \end{Bmatrix} \begin{Bmatrix} S_1' & 1/2 & S' \\ S_c'' & 1/2 & S_1 \end{Bmatrix} \begin{Bmatrix} L_1' & L'' & l_3 \\ L_c'' & L_1 & l_1 \end{Bmatrix} \langle l_6\|C^k\|l_3\rangle$$

$$\times\langle l_1\|C^k\|l_1\rangle R_k(l_1l_6;l_1l_3)(-1)^{L_1+L''+l_1+S''+2S_c'+l_3+3S_1+2S_c''}.$$

For the Coulomb interaction

$$|l_3^{n_3-1}[L_3'S_3']l_1'^{n_1+1}[L_1'S_1']l_2^{n_2}[L_2S_2]L''S''\rangle \to |l_3^{n_3}[L_3S_3]l_1'^{n_1-1}[L_c'S_c']l_2^{n_2}[L_2S_2][L_c'S_c']l_6L'S'\rangle, \tag{B4}$$

the Coulomb matrix element of time forward type is

$$\sum_{k\bar{L}} G^{l_1'^{n_1+1}[L_1'S_1']}_{l_1'^{n_1}[\bar{L}\bar{S}]} G^{l_1'^{n_1}[\bar{L}\bar{S}]}_{l_1'^{n_1-1}[L_c'S_c']} \frac{[\bar{L},\bar{S},L_1',S_1']^{1/2}\sqrt{n_1+1}\sqrt{n_1}}{[S']} \begin{Bmatrix} l_1 & l_3 & k \\ L'' & \bar{L} & L_1' \end{Bmatrix} \begin{Bmatrix} l_6 & l_1 & k \\ \bar{L} & L' & L_c' \end{Bmatrix} \langle l_6\|C^k\|l_1\rangle\langle l_3\|C^k\|l_1\rangle R_k(l_6l_3;l_1l_1)$$

$$\times(-1)^{k+2S'+2S_1'+l_3+L_1'+n_1+\bar{L}+L'+1+l_1+L_c'} + \sum_{k\bar{L}} G^{l_1'^{n_1+1}[L_1'S_1']}_{l_1'^{n_1}[\bar{L}\bar{S}]} G^{l_1'^{n_1}[\bar{L}_1\bar{S}_1]}_{l_1'^{n_1-1}[L_c'S_c']} \frac{[\bar{L}_1,\bar{S}_1,L_1',S_1']^{1/2}\sqrt{n_1+1}\sqrt{n_1}}{[S']} \begin{Bmatrix} l_1 & l_3 & k \\ L'' & \bar{L} & L_1' \end{Bmatrix} \begin{Bmatrix} l_6 & l_1 & k \\ \bar{L} & L' & L_c' \end{Bmatrix}$$

$$\times\langle l_6\|C^k\|l_1\rangle\langle l_3\|C^k\|l_1\rangle R_k(l_6l_3;l_1l_1)(-1)^{k+2S'+2S_1'+l_3+L_1'+n_1+\bar{L}+L'+1+l_1+L_c'}.$$

The exchange part of the Coulomb matrix element of time backward type is

$$-\sum_{kL_c''S_c''} G^{l_1'^{n_1+1}[L_1'S_1']}_{l_1^{n_1}[L_1S_1]} G^{l_1'^{n_1}[L_1S_1]}_{l_1'^{n_1-1}[L_c'S_c']} [L_c'',S_c''][L,S,L_1',S_1']^{1/2}\sqrt{n_1+1} \begin{Bmatrix} L' & L_c' & l_6 \\ L_c'' & L & l_3 \\ l_1 & l_1 & k \end{Bmatrix} \begin{Bmatrix} S_c' & 1/2 & S' \\ S_c'' & 1/2 & S \end{Bmatrix} \begin{Bmatrix} S_1' & 1/2 & S'' \\ S_c'' & 1/2 & S_1 \end{Bmatrix} \begin{Bmatrix} L_1' & L'' & l_3 \\ L_c'' & L_1 & l_1 \end{Bmatrix} \langle l_6\|C^k\|l_3\rangle$$

$$\times\langle l_1\|C^k\|l_1\rangle R_k(l_1l_6;l_1l_3)(-1)^{L''+2S+n_1+L+2S_c'+1}.$$

[1] P. L. Altick and A. E. Glassgold, Phys. Rev. **133**, A632 (1964).
[2] M. Ya. Amusia and N. A. Cherepkov, Case Stud. At. Phys. **5**, 47 (1974).
[3] A. F. Starace, J. Phys. B **7**, 14 (1974).
[4] M. Ya. Amusia *et al.*, Sov. Phys. JETP **33**, 90 (1971).
[5] N. A. Cherepkov and L. V. Chernysheva, Phys. Lett. **60A**, 103 (1977).
[6] G. A. Vesnicheva *et al.*, Sov. Phys. Tech. Phys. **31**, 402 (1986).
[7] Zhifan Chen and A. Z. Msezane, Phys. Rev. A **72**, 050702(R) (2005).
[8] Zhifan Chen and A. Z. Msezane, J. Phys. B **39**, 4355 (2006).
[9] S. B. Whitfield, K. Kehoe, R. Wehlitz, M. O. Krause, and C. D. Caldwell, Phys. Rev. A **64**, 022701 (2001); S. B. Whitfield, T. Myers, M. Bjelland, R. Wehlitz, J. Jimenez-Mier, P. Olalde-Velasco, and M. O. Krause, *ibid.* **66**, 060701(R) (2002).
[10] Z. Altun and S. T. Manson, Phys. Rev. A **59**, 3576 (1999); **61**, 030702(R) (2000).
[11] B. Sonntag and P. Zimmermann, Rep. Prog. Phys. **55**, 911 (1992).
[12] M. Martins, J. Phys. B **35**, L223 (2002).
[13] I. I. Sobel'man, *Introduction to the Theory of Atomic Spectra* (Pergamon, New York, 1972).